

SUPPORTING INFORMATION

Antidiabetic in vitro and in vivo evaluation of cyclodipeptides isolated from *Pseudomonas fluorescens* IB-MR-66e

M. Lozano-González ^a, B. Ovalle-Magallanes ^a, M. Rangel-Grimaldo ^a, Susana de la Torre-Zavala ^b, Lilia G. Noriega ^c, Claudia Tovar-Palacio ^d, Armando R. Tovar ^c, and R. Mata*^a

- a. Facultad de Química, Departamento de Farmacia, Universidad Nacional Autónoma de México, Ciudad de México, México.
- b. Instituto de Biotecnología, Universidad Autónoma de Nuevo León, Monterrey, México.
- c. Instituto Nacional de Ciencias Médicas y Nutrición "Salvador Zubirán", Departamento de Fisiología de la Nutrición, Ciudad de México, México.
- d. Instituto Nacional de Ciencias Médicas y Nutrición "Salvador Zubirán", Departamento de Nefrología y Metabolismo Mineral, Ciudad de México, México

INDEX

1.1 Synthesis and characterization of cyclodipeptides

1.2 Inhibition of α -glucosidases

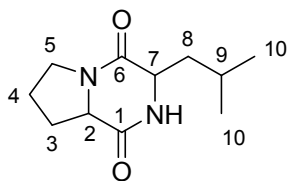
2.1 Theory calculation

3.1 Western Blot analysis

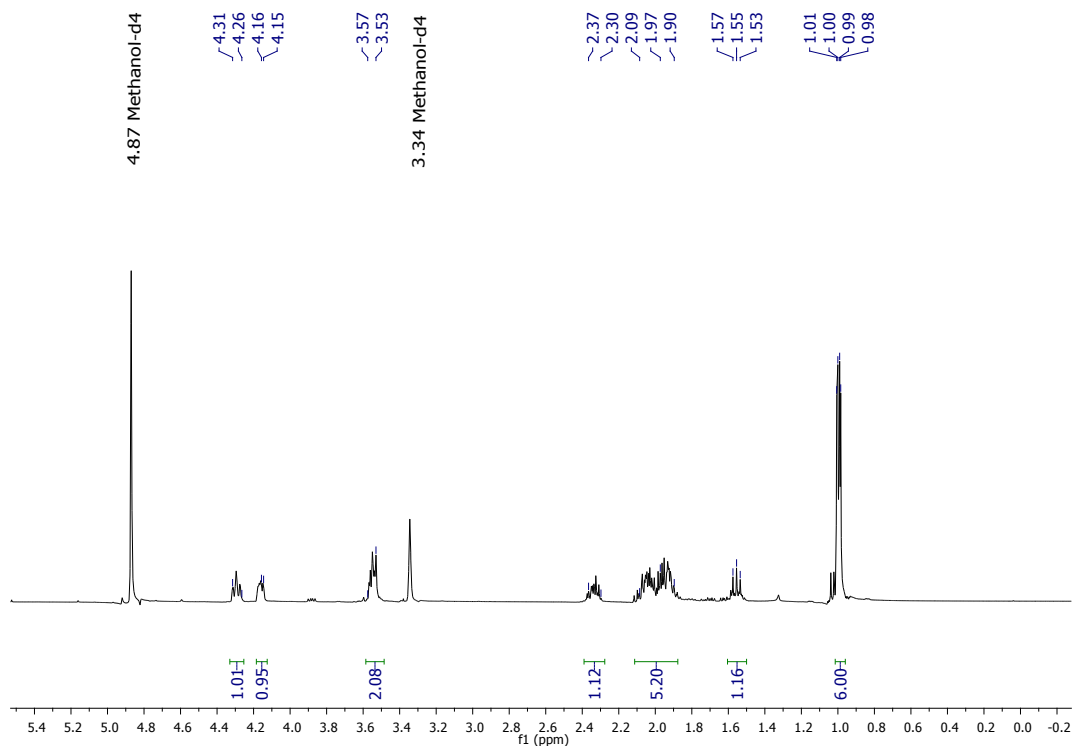
1.1 Synthesis and characterization of cyclodipeptides

The general procedure for peptide coupling was N,N-Diisopropylethylamine (6.0 mmol), N-Boc-L- aminoacid (3.0 mmol) and (2-(1H-benzotriazol-1-yl)-1,1,3,3-tetramethyluronium hexafluorophosphate (HBTU) (3.5 mmol) were added to a solution of L-proline methyl ester hydrochloride (3.0 mmol) in *N,N*-Dimethylformamide (DMF). The reaction mixture was stirred at room temperature 12h. The DMF was removed in vacuo and the residue was diluted in EtOAc, washed with NaHCO₃, brine, dried over anhydrous Na₂SO₄ and filtered. The solvent was evaporated in vacuo. The resulting crude product was purified by column chromatography using silica gel (ethyl acetate/hexane, 1:1) obtaining the desired linear dipeptide.

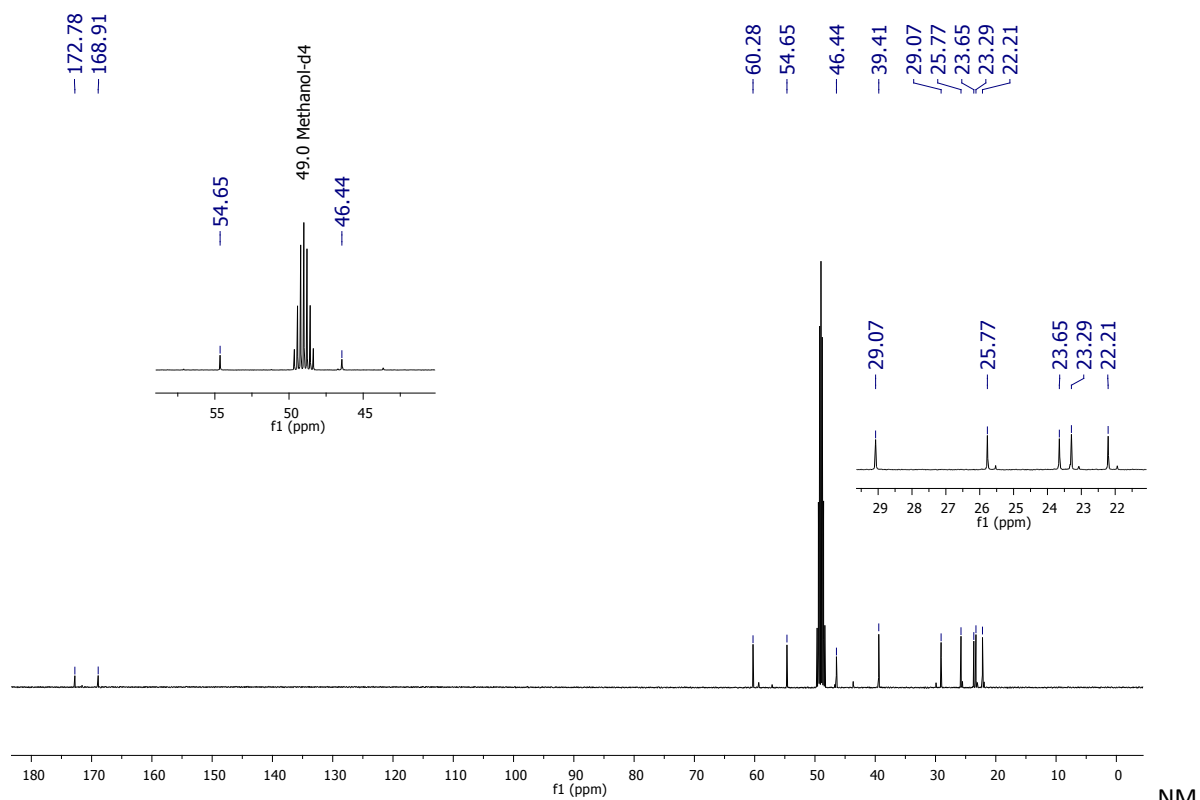
N-Boc-aminoacid-L-proline methyl ester held in a borosilicate glass, silicon carbide 10 mL vial with magnetic bar was suspended in 5mL of water. The reaction vessel was introduced in a monowave 300 Anton Paar 100°C during 1h30min. Water was evaporated in vacuo, the remaining residue was purified by column chromatography using silica gel (MeOH/CH₂Cl₂, 30:70).



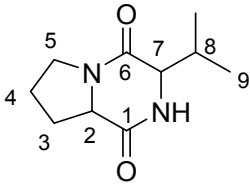
Compound 1.- Synthetic $[\alpha]_D = -0.184^\circ$ (c 1.68, MeOH) Isolated $[\alpha]_D = -0.028^\circ$ (c 0.28, MeOH) D **NMR ^1H** (400 MHz, $\text{CD}_3\text{OD-d}_4$) δ (ppm): 0.99(d, 3H, H10, $J = 6.7\text{Hz}$), 1.00 (d, 3H, H10, $J = 7.1\text{ Hz}$), 1.56(m, 2H,H8), 1.99 (m, 5H, H4, H8, H3), 2.33 (m, 3H, H3), 3.54 (m,2H,H5) , 4.16 (m,1H, H7), 4.29 (m, 1H, H2). **NMR ^{13}C** (100MHz, $\text{CD}_3\text{OD-d}_4$) δ (ppm): 22.2 (C10), 23.3 (C10), 23.6 (C4), 25.8 (C9), 29.1 (C3), 39.4 (C8), 46.4 (C5), 54.7 (C7), 60.28 (C2), 168.91(C6), 172.78 (C1). **HRESIMS:** 211.14410 $[\text{M}+\text{H}]^+$ $\text{C}_{11}\text{H}_{19}\text{N}_2\text{O}_2$.



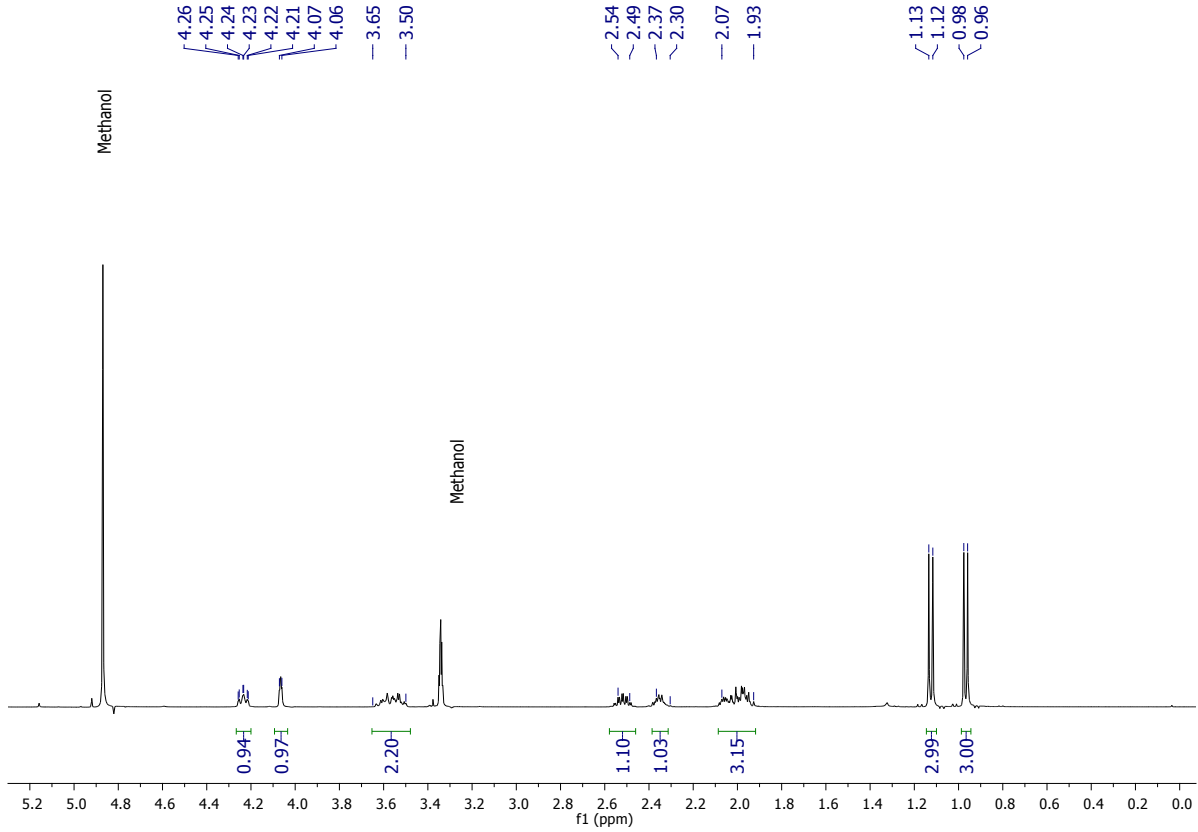
NMR ^1H (400 MHz, $\text{CD}_3\text{OD-d}_4$) **Compound 1.**



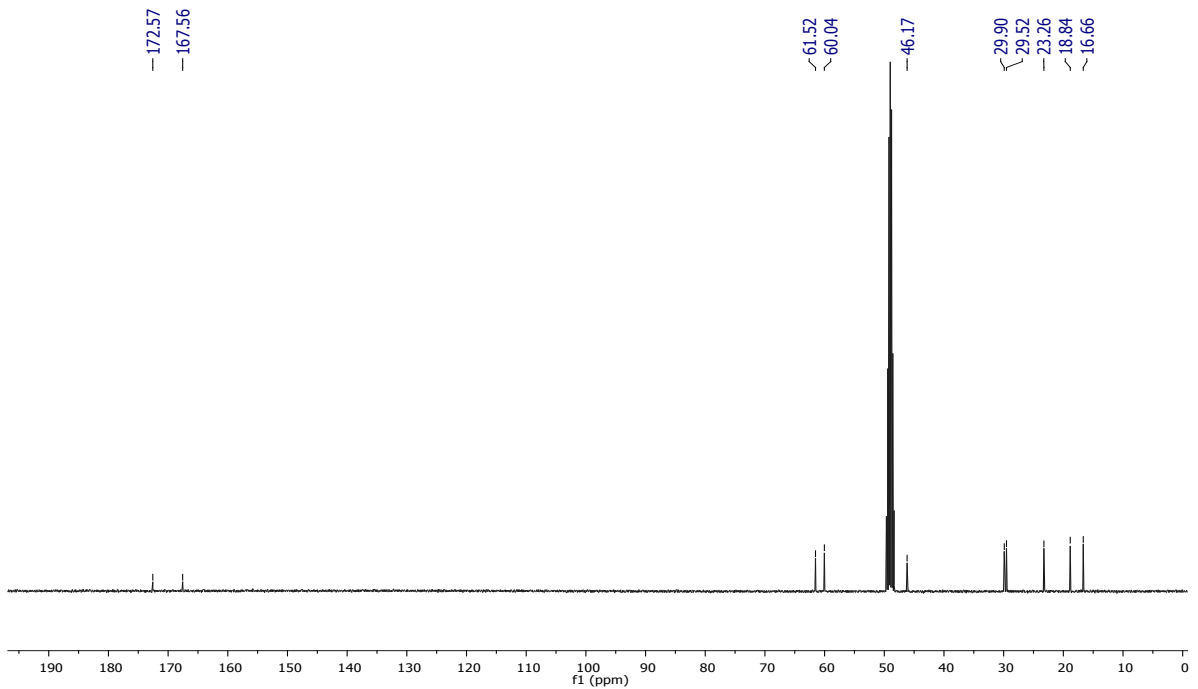
R ^{13}C (100 MHz, $\text{CD}_3\text{OD-d}_4$) **Compound 1.**



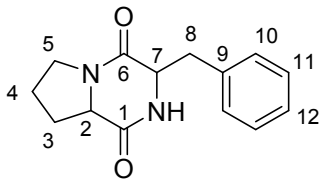
Compound 2. Synthetic $[\alpha]_D = -0.118^\circ$ (c 0.78, MeOH) **NMR ^1H** (400 MHz, $\text{CD}_3\text{OD-d}_4$) δ (ppm): 0.97(d, 3H, H9, $J = 6.9\text{Hz}$), 1.13 (d, 3H, H9, $J = 7.2\text{Hz}$), 2.01 (m, 3H, H3, H4), 2.34 (m, 1H, H3), 2.52(dq, 1H, H8, $J = 2.5\text{Hz}$, $J = 7.1\text{Hz}$), 3.56 (m, 2H, H5), 4.07 (m, 1H, H7, $J = 2.2\text{Hz}$), 4.24 (m, 1H, H2). **NMR ^{13}C** (100MHz, $\text{CD}_3\text{OD-d}_4$) δ (ppm): 16.7 (C9), 18.8 (C9), 23.3 (C4) 29.5 (C3), 29.9 (C8), 46.2 (C5), 60.0 (C7), 61.5 (C2), 167.6 (C6), 172.6 (C1). **HRESIMS:** 197.12845 $[\text{M}+\text{H}]^+$ $\text{C}_{10}\text{H}_{17}\text{N}_2\text{O}_2$.



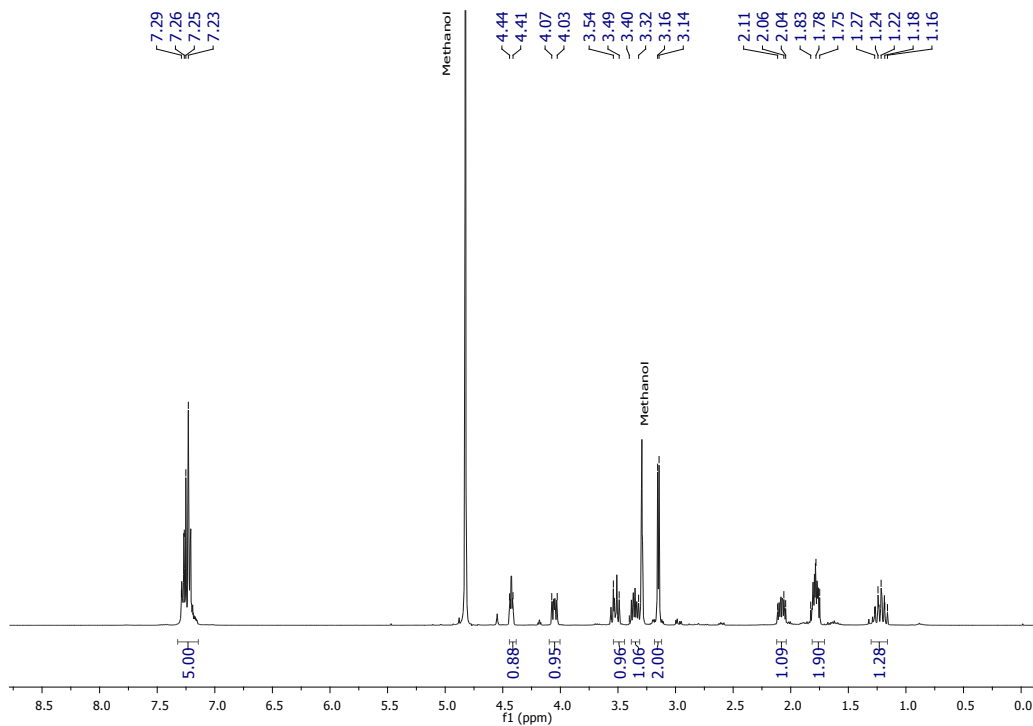
NMR ^1H (400 MHz, $\text{CD}_3\text{OD-d}_4$) **Compound 2.**



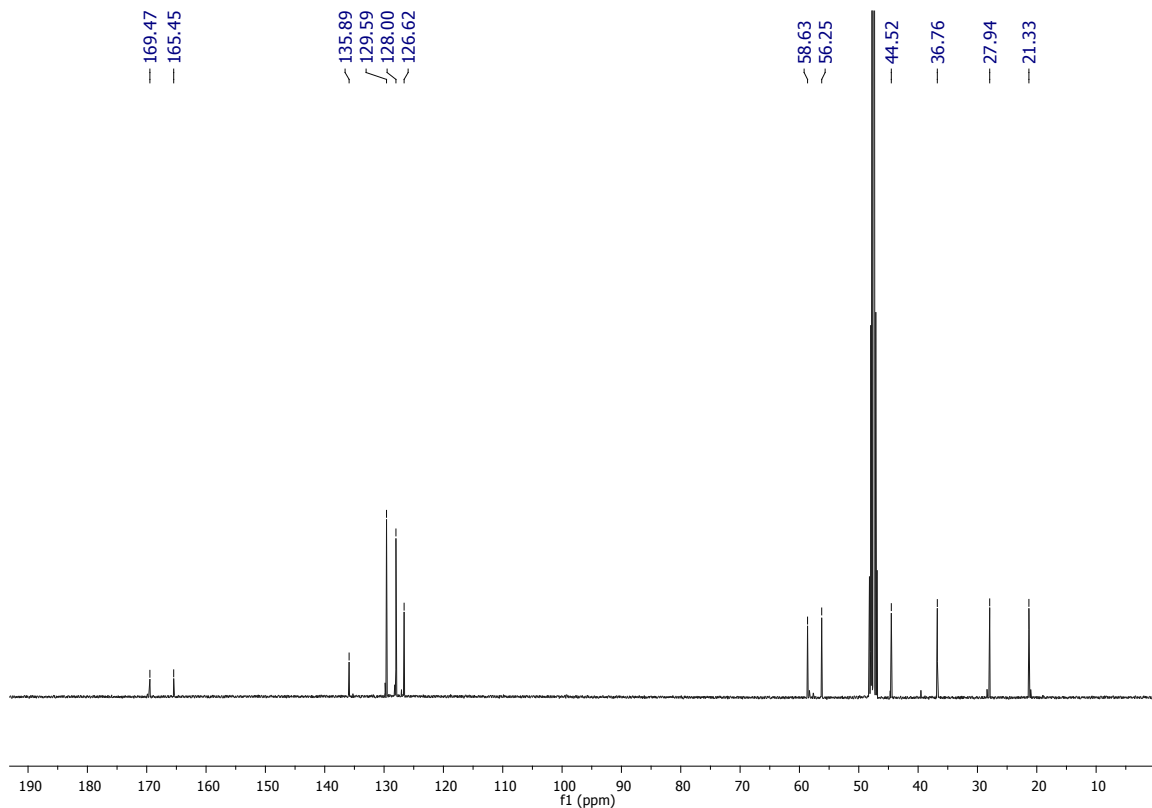
NMR ^{13}C (100 MHz, $\text{CD}_3\text{OD-d}_4$) **Compound 2.**



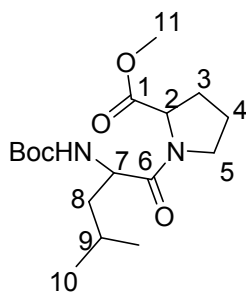
Compound 3. NMR ^1H (400 MHz, $\text{CD}_3\text{OD-d}_4$) δ (ppm):, 1.18 (m, 1H, H4), 1.78 (m, 2H, H4, H3), 2.06 (m, 1H, H3), 3.15 (d, 2H, H8, $J = 5$ Hz), 3.37 (m, 1H, H5), 3.53 (m, 1H, H5), 4.05 (dd, 1H, H7, $J = 10.8, 6.4, 1.8$ Hz), 4.41 (t, 1H, H2, $J = 4.6$ Hz, H-3), 7.4 (m, 5H, H9, H10, H11, H12). NMR ^{13}C (100 MHz, $\text{CD}_3\text{OD-d}_4$) δ (ppm): 21.3 (C4), 27.9 (C3), 36.8 (C8), 44.5 (C5), 56.3 (C7), 58.6 (C2), 126.6 (C12), 128.0 (C10), 129.6 (C11), 135.9 (C9), 165.5 (C6), 169.5 (C1). HRESIMS: 245.12845 $[\text{M}+\text{H}]^+$ $\text{C}_{14}\text{H}_{17}\text{N}_2\text{O}_2$.



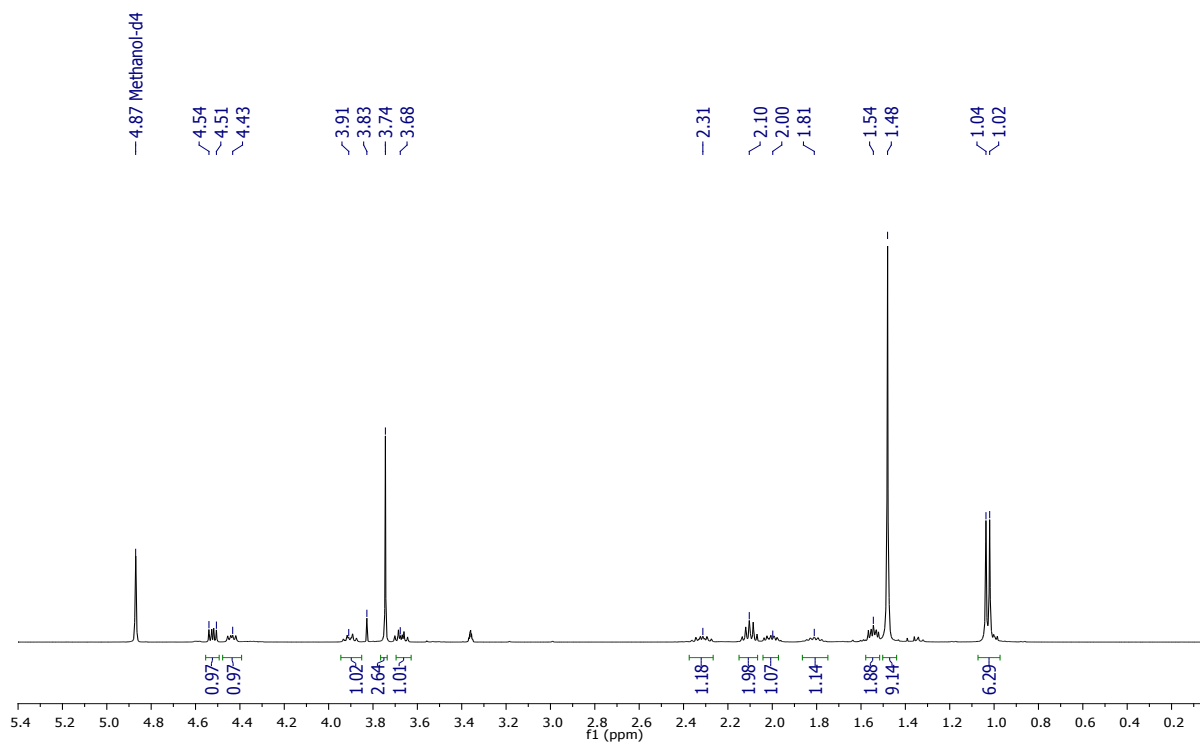
NMR ^1H (400 MHz, $\text{CD}_3\text{OD-d}_4$) **Compound 3.**



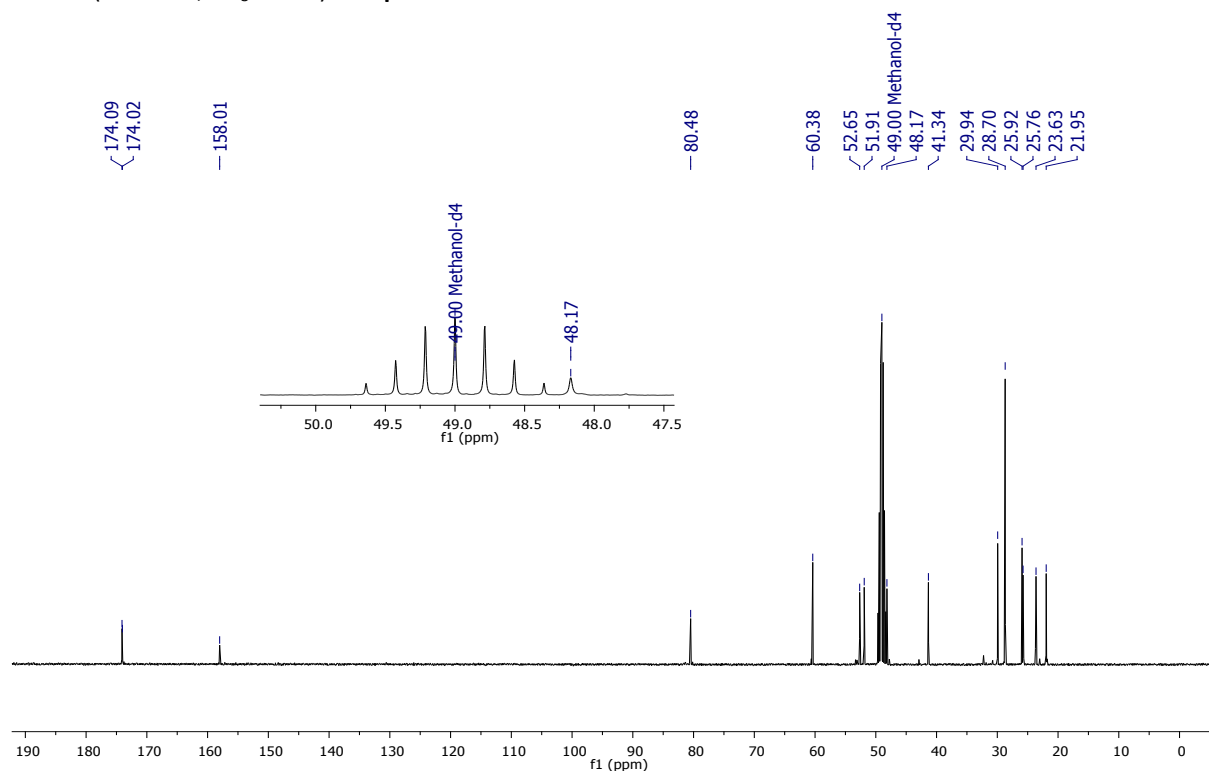
NMR ^{13}C (100 MHz, $\text{CD}_3\text{OD-d}_4$) **Compound 3.**



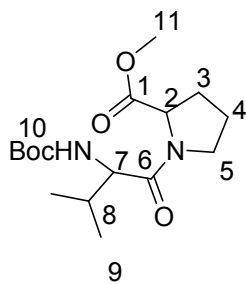
Compound 1a. NMR ¹H (400 MHz, CD₃OD-d₄) δ(ppm): 1.03 (d, 6H, H10, *J*= 8Hz), 1.48 (s, 9H, H10Boc), 1.54 (m, 2H, H9,H8), 1.81 (m, 1H, H8), 2.00 (m, 1H, H4), 2.10(q, 2H, H3,H4), 2.31 (m, 1H, H3), 3.68(m, 1H,H5), 3.74 (s, 3H, H11), 3.83 (s, NH), 3.91 (m, 1H, H5), 4.43 (m, 1H, H7), 4.53 (dd, 1H, H2, *J*= 8 Hz, *J*= 8 Hz). **NMR ¹³C** (100MHz, CD₃OD-d₄) δ(ppm): 21.9 (C10), 23.6 (C10), 25.8 (C9), 25.9 (C4), 28.7 (CBoc), 29.9(C3), 41.3 (C8), 48.2 (C5), 51.9 (C11), 52.7 (C7), 60.4 (C2), 80.5 (CBoc), 158.0 (COBoc), 174.0 (C6), 174.1 (C1).



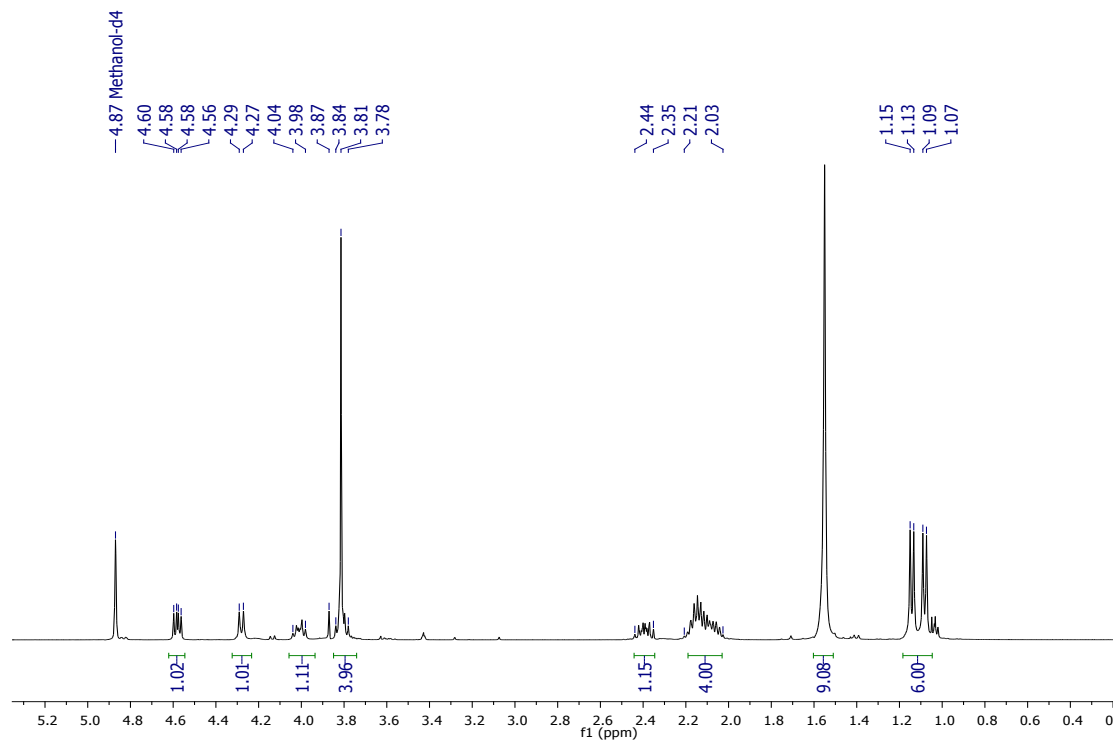
NMR ¹H (400 MHz, CD₃OD-d₄) **Compound 1a.**



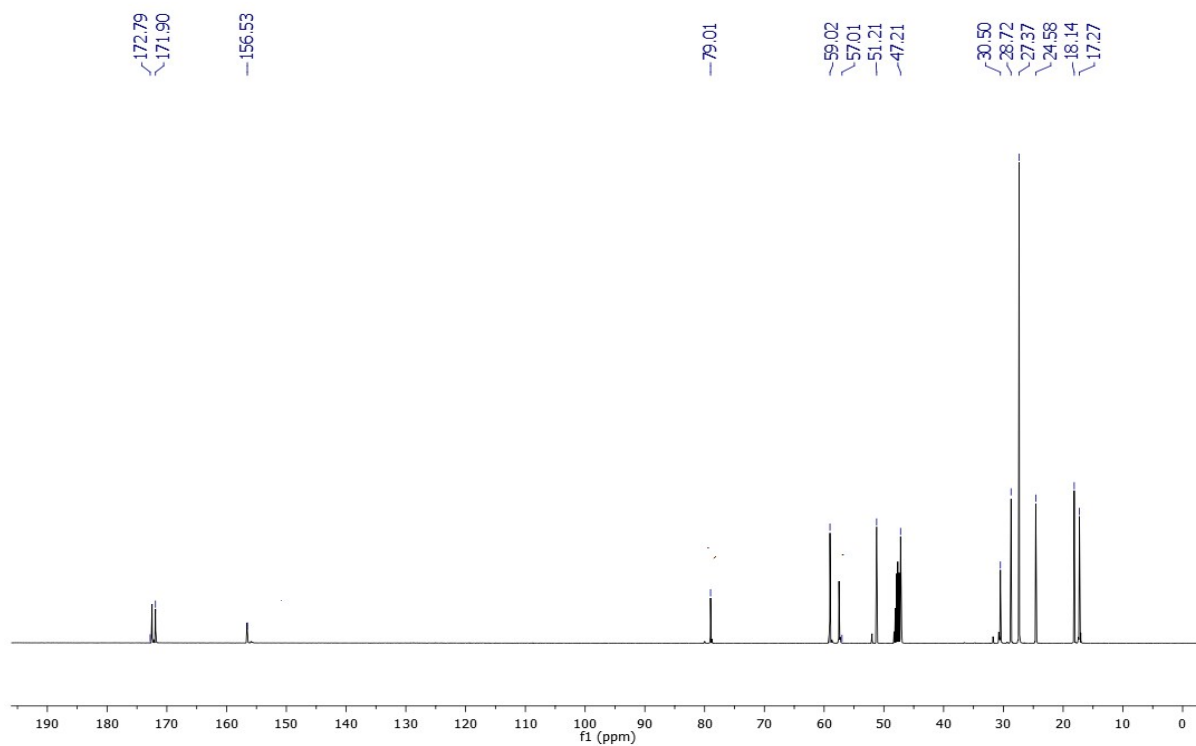
NMR ¹³C (100 MHz, CD₃OD-d₄) **Compound 1a.**



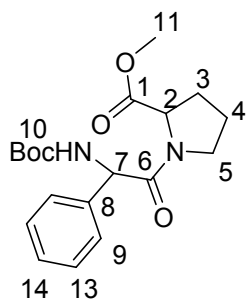
Compound 2a. NMR ^1H (400 MHz, $\text{CD}_3\text{OD-d}_4$) δ (ppm): 1.08(d, 3H, H9, $J=8\text{Hz}$), 1.14 (d, 3H, H9, $J=8\text{Hz}$), 2.12 (m, 4H, H8, H4, H3), 2.40 (m, 1H, H3), 3.81(s, 3H, H11), 3.82 (m, 1H, H5), 3.87 (s, NH), 4.01 (m, 1H, H5), 4.28 (d, 1H, H7, $J=8\text{Hz}$), 4.58 (dd, 1H, H2, $J=8\text{Hz}$, $J=8\text{Hz}$). **NMR ^{13}C** (100MHz, $\text{CD}_3\text{OD-d}_4$) δ (ppm): 17.3 (C9), 18.1 (C9), 24.6 (C4), 27.4 (CBoc), 28.7 (C3), 30.5 (C8), 47.2 (C5), 51.2 (C11), 57.0 (C7), 59.0 (C2), 79.0 (CBoc), 156.5 (CBoc), 171.9 (C1), 172.8 (C6).



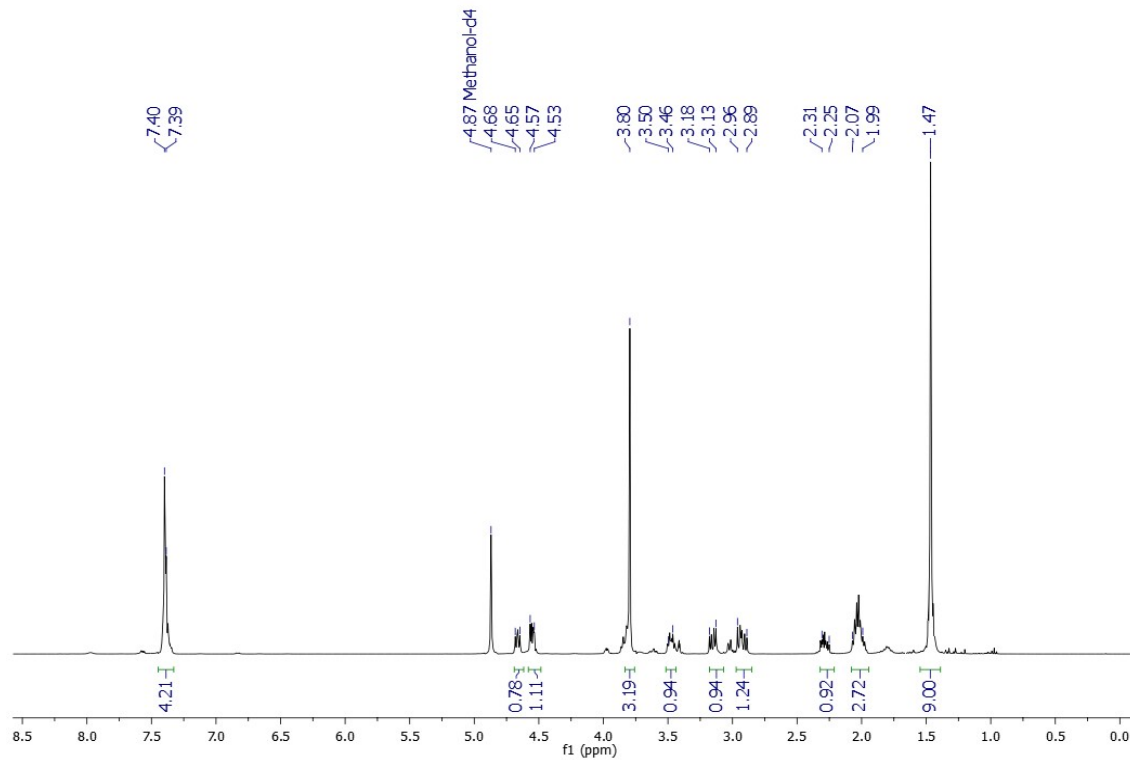
NMR ^1H (400 MHz, $\text{CD}_3\text{OD-d}_4$) **Compound 2a.**



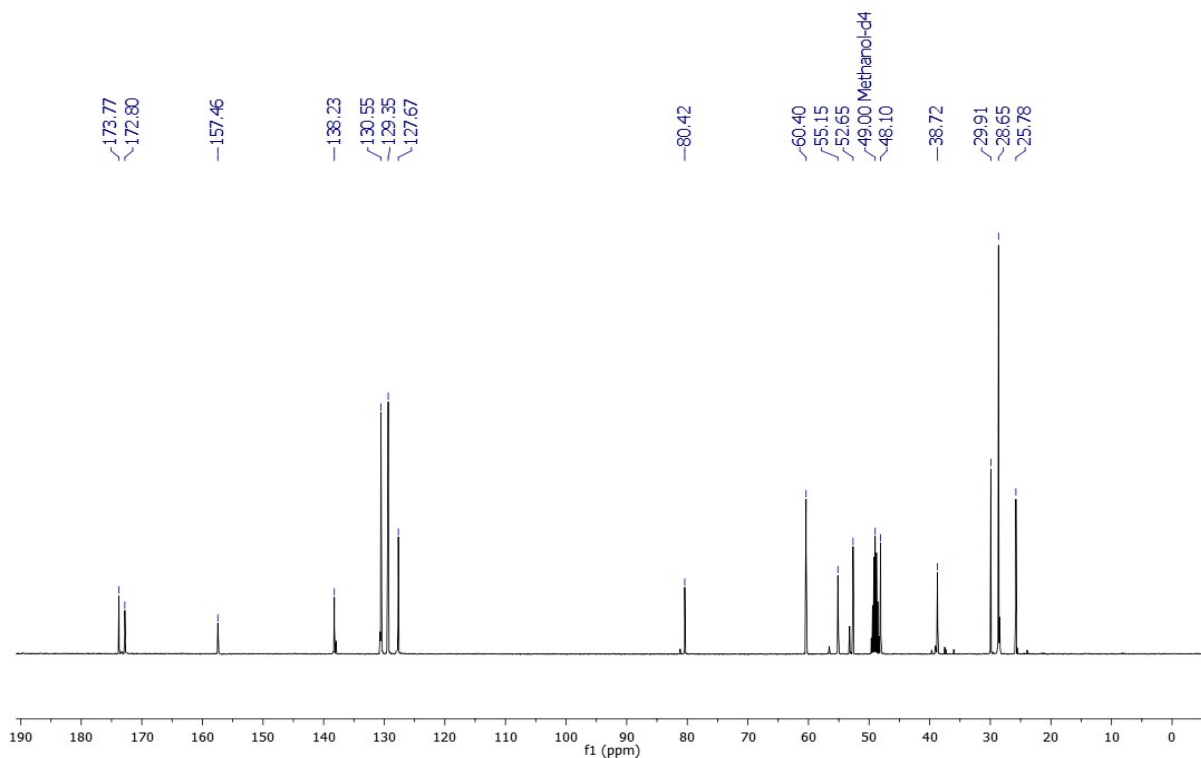
NMR ^{13}C (100 MHz, $\text{CD}_3\text{OD-d}_4$) **Compound 2a.**



Compound 3a. NMR ^1H (400 MHz, $\text{CD}_3\text{OD-d}_4$) δ (ppm): 1.47 (s, 9H, H10Boc), 2.03 (m, 2H, H4), 2.30 (m, 1H, H3), 2.93 (m, 1H, H3), 3.16 (m, 1H, H5), 3.48 (m, 1H, H5), 3.80 (s, 3H, H11), 4.55 (m, 1H, H7), 4.67 (t, 1H, H2), 7.39 (m, 5H, H9, H13, H14). **NMR ^{13}C** (100MHz, $\text{CD}_3\text{OD-d}_4$) δ (ppm): 25.8 (C4), 28.7 (CBoc), 29.9 (C10Boc), 38.7 (C3), 48.1 (C5), 52.7 (C11), 55.2 (C7), 60.4 (C2), 80.4 (CBoc), 127.7 (C14), 129.4 (C13), 130.6 (C9), 138.2 (C8), 157.5 (CBoc), 172.8 (C1), 173.8 (C6).



NMR ^1H (400 MHz, $\text{CD}_3\text{OD-d}_4$) **Compound 3a.**



NMR ^{13}C (100 MHz, $\text{CD}_3\text{OD-d}_4$) **Compound 3a.**

1.2 Inhibition of α -glucosidases

The bacterial extract, fractions, compounds, and acarbose (positive control) were dissolved in MeOH. Aliquots of 0–40 μ L of testing materials (triplicated) were incubated for 10 min with 20 μ L of enzyme stock solution (0.4 U mL⁻¹ in phosphate buffer solution 100 mM, pH 7). After incubation, 10 μ L of substrate (*p*NPG 5 mM) was added and further incubated for 30 min at 37°C, and the absorbance of each sample was determined. The inhibitory activity was expressed as IC₅₀ as previously reported. (M. Rangel-Grimaldo, I. Rivero-Cruz, A. Madariaga-Mazón, M. Figueroa, R. Mata, J. Nat. Prod., 2017, 80, 582-587.)

Table 2. Inhibitory effect of the metabolites of the bacteria studied in the enzymes of *Saccharomyces cerevisiae*, NA: No activity, [] Concentration.

Sample	[]	% inhibition of α -glucosidase of <i>S. cerevisiae</i>	IC ₅₀ (mM)
Extract <i>P. fluorescens</i>	1000 ppm	56	-
Compound 1	15mM	95	4.6 \pm 0.2
Compound 2	10mM	96	3.2 \pm 0.5
Compound 3	10mM	94	3.4 \pm 0.6
Precursor 1a	10mM	NA	-
Precursor 2a	10mM	NA	-
Precursor 3a	10mM	NA	-
Acarbose	5mM	97	1.6+0.1

2.1 Theory calculation

The minimized structures for docking simulations were prepared using Autodock Tools package v1.5.4 (ADT, <http://mgltools.scripps.edu/>). For metabolites, addition of Gasteiger charges and number of torsions were set, and non-polar hydrogens were merged. The crystallographic structure of alpha-glucosidase from yeast was obtained from the Protein Data Bank (RCSB; pdb code 3A4A). For the receptor all hydrogens (polar and nonpolar) and Kollman charges were added, and solvation parameters were assigned by default.

Molecular docking studies were achieved with AutoDock 4.2.6. First, a blind docking was performed to establish the common site of interaction of the metabolites with the alpha-glucosidase. The search space for this preliminary docking was defined as a box size of $54 \times 68 \times 68$ Å in the x, y and z dimensions, with a grid spacing of 1.0 Å and the macromolecule set at the centre of the box. The default parameters of exhaustiveness and number of modes were not altered. Next, a refine docking was performed with a smaller box of searching space ($30 \times 25 \times 25$ Å, and 1.0 Å of grid spacing), setting as the centre of the grid box the lower state pose obtained from the blind docking. The conformational states from the docking simulations were analysed using the AutoDockTools program, which also identified the H-bonds and van der Waals interactions between the catalytic site of α -glucosidase and the ligand. The predicted docked complexes (protein-ligand) were those conformations showing the lowest binding energy. The estimated inhibition constant (K_i) was calculated from the docking energy displayed by AutoDock following the equation $K_i = \exp(\Delta G \times 1000 / RT)$, where ΔG is the docking energy, R is the universal constant of ideal gas (1.98719 cal K⁻¹ mol⁻¹), and T is the temperature (298.15 K). Preparation of the figures was accomplished with PyMOL visualization tool (The PyMOL Molecular Graphics System, Version 1.7.4 Schrödinger, LLC) and Discovery Studio.

3.1 Western Blot analysis

Frozen liver, adipose tissue and gastrocnemius muscle were homogenized in lysis buffer (50 mM Tris-HCl, 150 mM NaCl, 1 mM EDTA, 5 mM Na₄P₂O₇, 1 mM Na₃VO₄, 50 mM NaF and 1% NP-40) with protease inhibitor cocktail (Complete, Roche). Protein concentration was determined using the DC protein assay kit (Bio-Rad Laboratories, Richmond, CA). Tissue lysates (20 µg) were combined with Laemmli sample buffer and separated by SDS-PAGE. After electrophoretic separation, the proteins were electrotransferred to a PVDF membrane using a Mini Trans-Blot Electrophoretic Transfer Cell (Bio-Rad), blocked and incubated overnight at 4°C with the anti-AKT (sc-8312, Santa Cruz), anti-phospho-AKT (9018, Cell signalling) and anti-actin antibody (sc-1615, Santa Cruz). Band detection was carried out using a chemiluminescent Western blotting kit (Immobilon Western Chemiluminescent HRP Substrate, Millipore). Digital images of the membranes were obtained by a ChemiDoc MP densitometer and processed by Image Lab software (Bio-Rad, Hercules, CA, USA). Results are reported relative to Akt and β-actin.

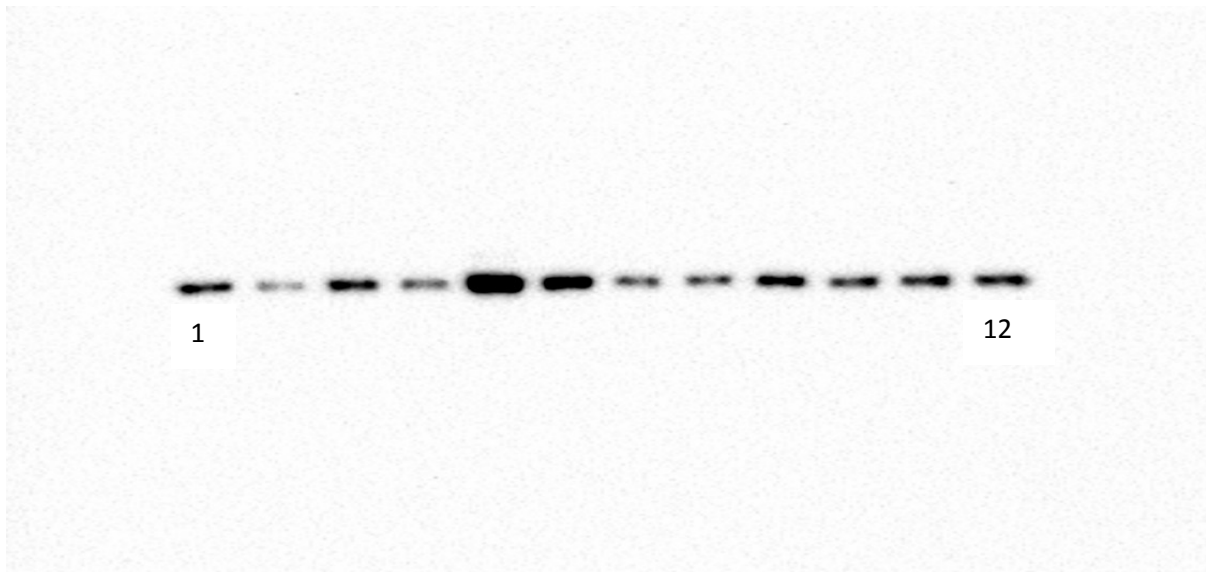


Figure 2. Representative blot of p-Akt from adipose tissue. From left to right (1→12), wells 1-3: control; 4-6: insulin; 7-9: insulin + 1. Last three wells represent triplicate of a DKP not included in the paper.

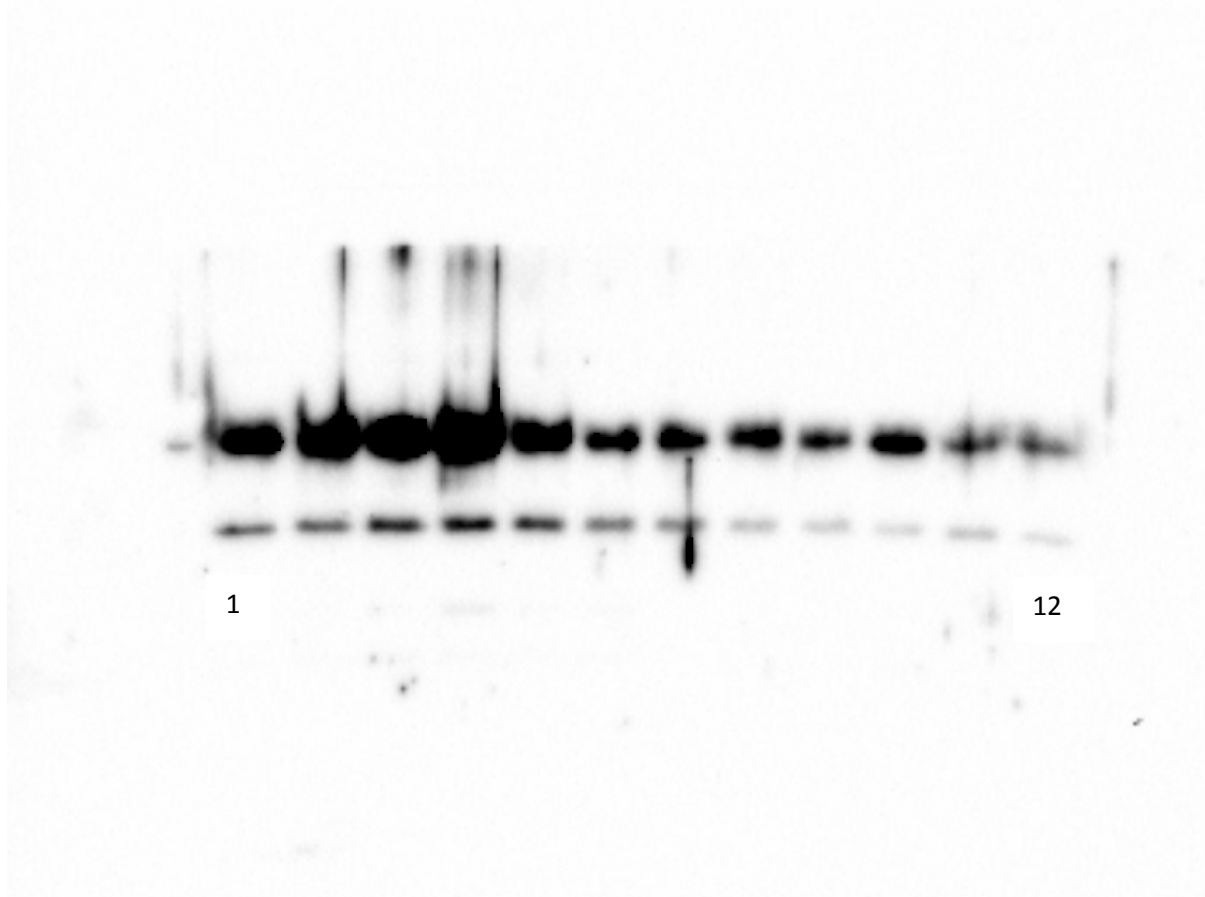


Figure 3. Representative blot of Akt from adipose tissue. From left to right (1→12), wells 1-3: control; 4-6: insulin; 7-9: insulin + **1**. Last three wells represent triplicate of a DKP not included in the paper. Blots on the lower part correspond to Akt isoform at 56 kDa.

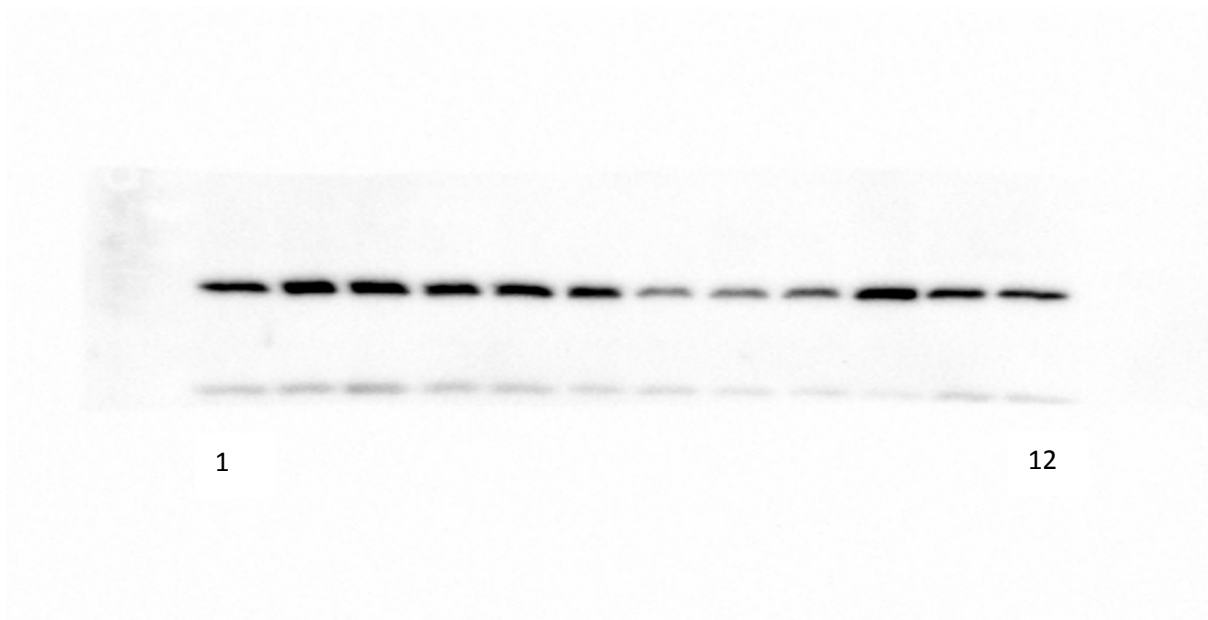
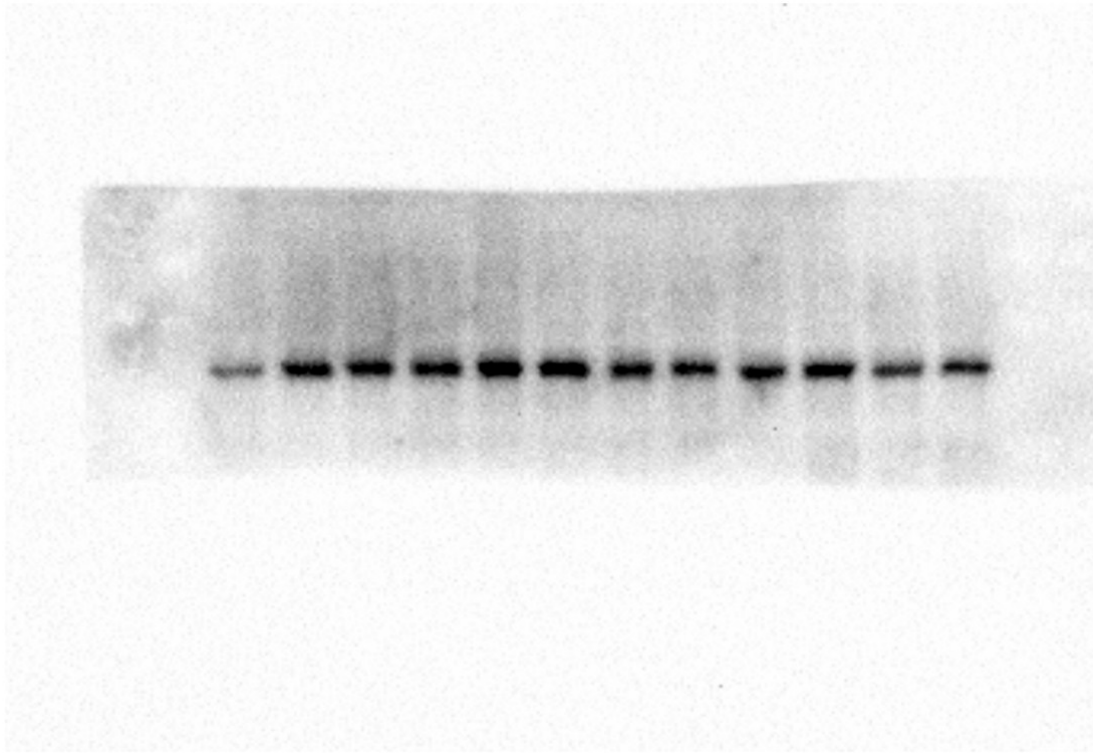


Figure 4. Representative blot of actin from adipose tissue. From left to right (1→12), wells 1-3: control; 4-6: insulin; 7-9: insulin + **1**. Last three wells represent triplicate of a DKP not included in the paper. Blots on the lower part correspond to proteins of lower kDa.



12

Figure 5. Representative blot of p-Akt from liver. From left to right (1→12), wells 1-3: control; 4-6: insulin; 7-9: insulin + **1**. Last three wells represent triplicate of a DKP not included in the paper

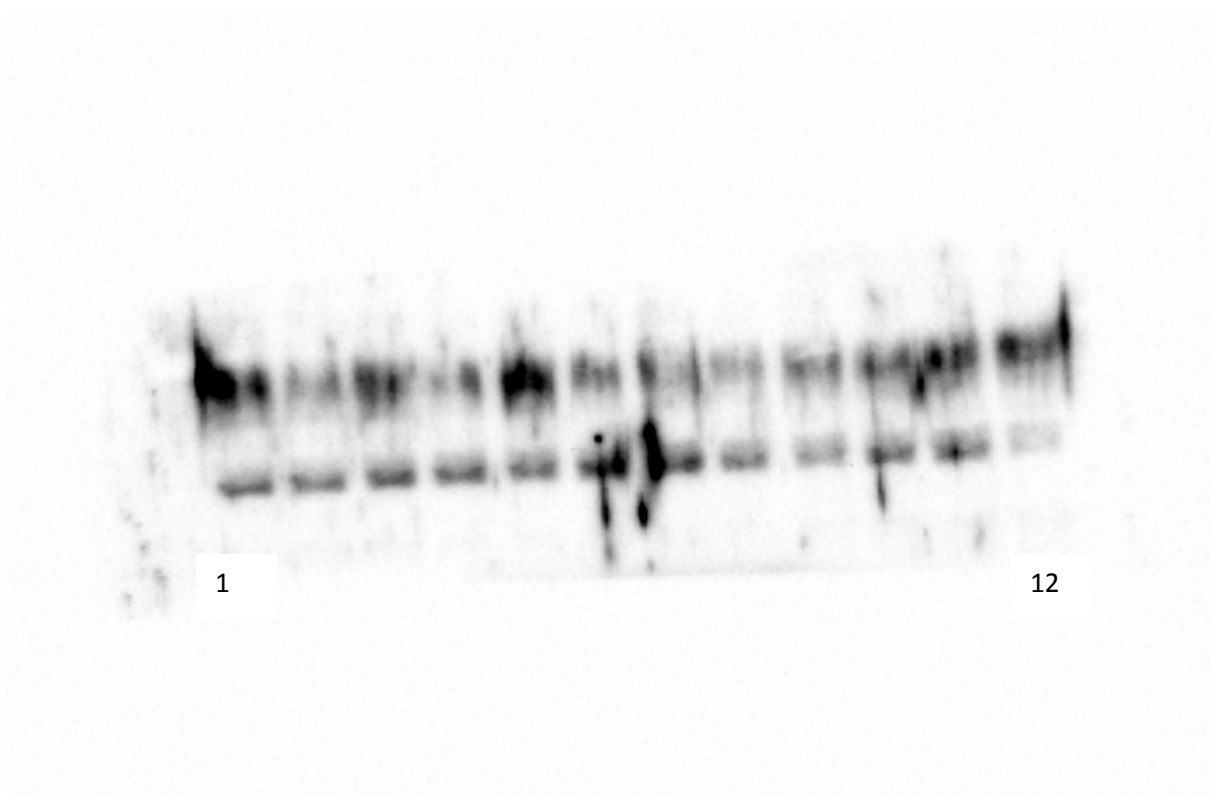


Figure 6. Representative blot of Akt from liver. From left to right (1→12), wells 1-3: control; 4-6: insulin; 7-9: insulin + **1**. Last three wells represent triplicate of a DKP not included in the paper. Blots on the upper part were not quantified.

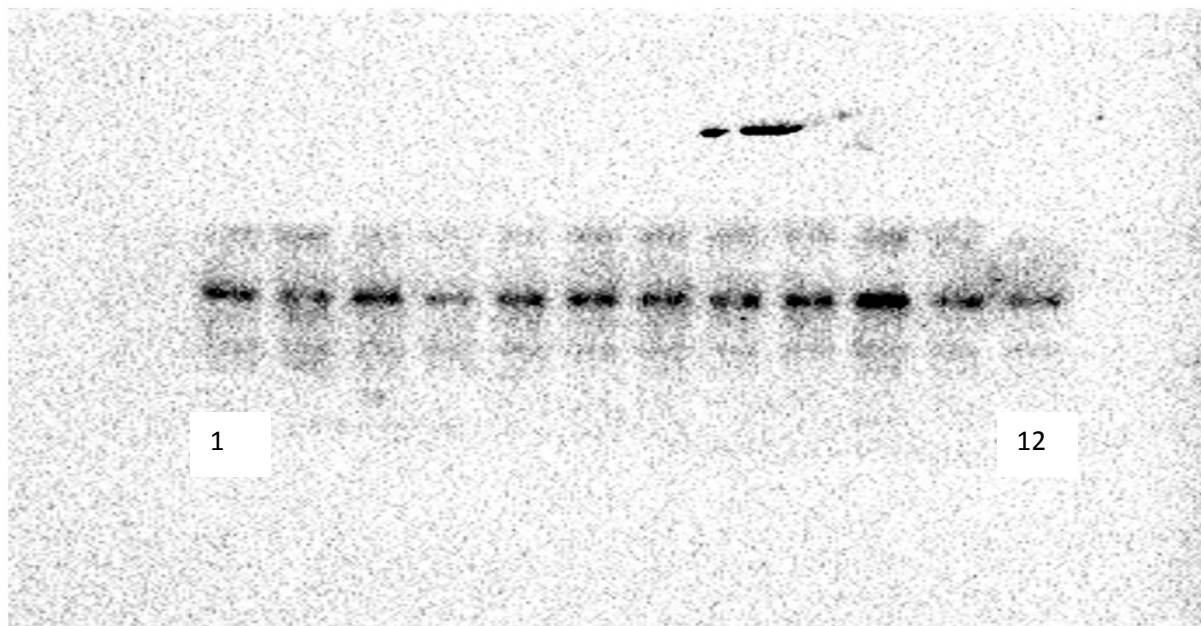


Figure 7. Representative blot of actin from liver. From left to right (1→12), wells 1-3: control; 4-6: insulin; 7-9: insulin + **1**. Last three wells represent triplicate of a DKP not included in the paper.

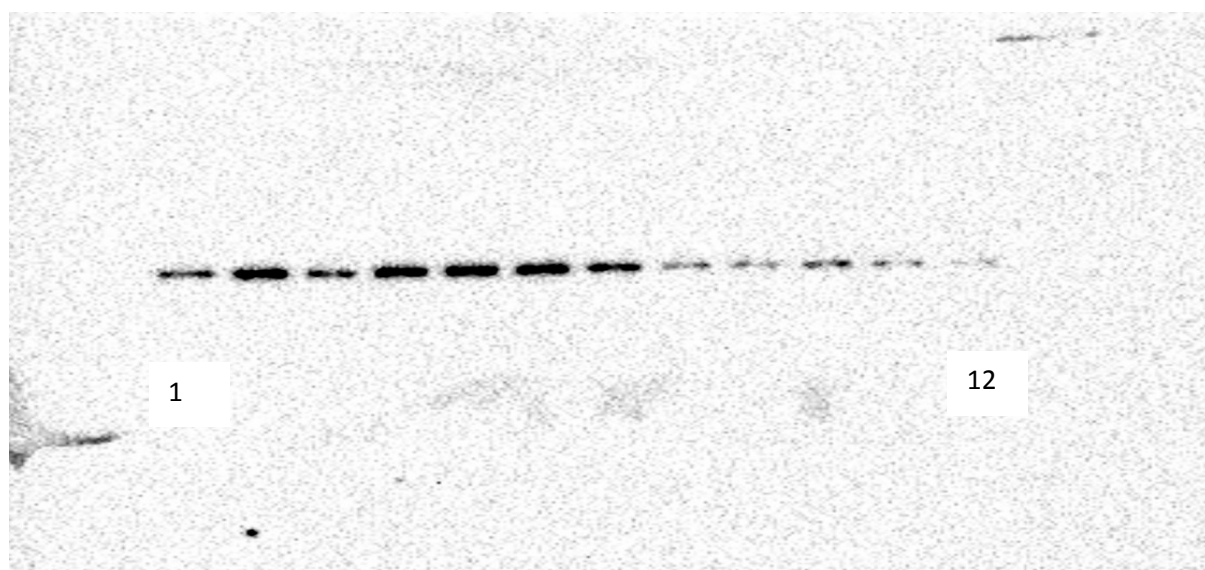


Figure 8. Representative blot of p-Akt from muscle. From left to right (1→12), wells 1-3: control; 4-6: insulin; 7-9: insulin + **1**. Last three wells represent triplicate of a DKP not included in the paper.

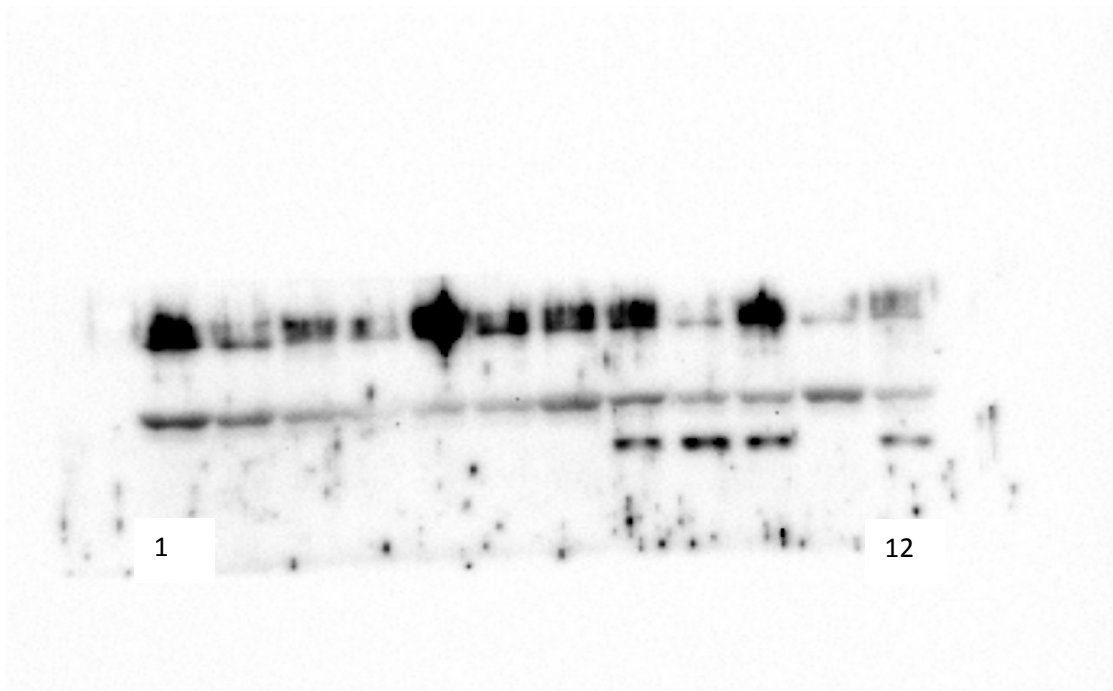


Figure 9. Representative blot of Akt from muscle t muscle. From left to right (1→12), wells 1-3: control; 4-6: insulin; 7-9: insulin + **1**. Last three wells represent triplicate of a DKP not included in the paper.

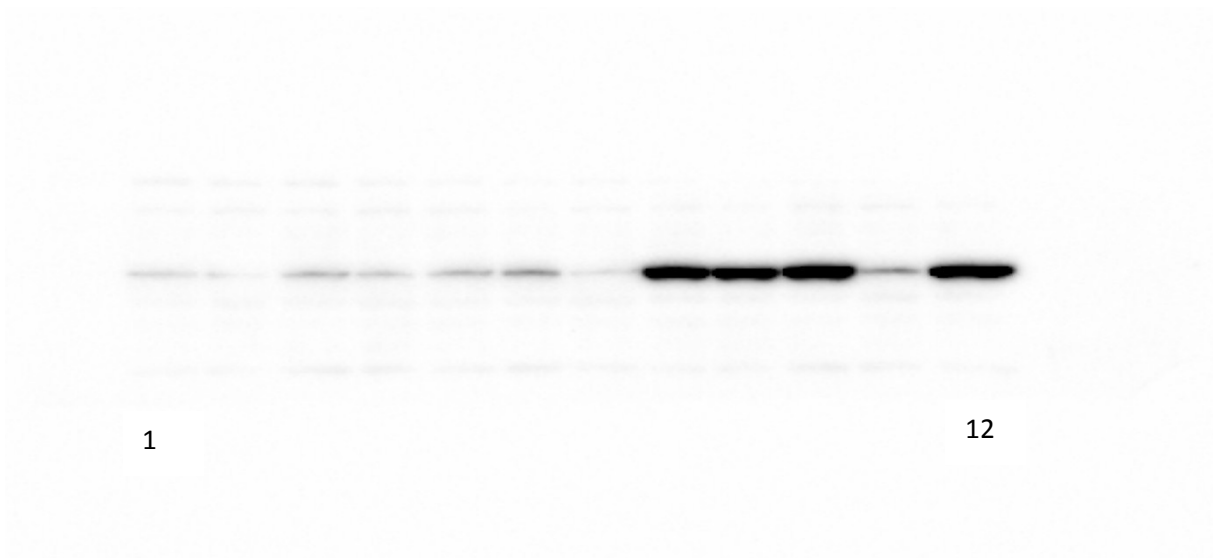


Figure 10. Representative blot of actin from muscle t muscle. From left to right (1→12), wells 1-3: control; 4-6: insulin; 7-9: insulin + **1**. Last three wells represent triplicate of a DKP not included in the paper.